Am J Transl Res 2019;11(9):6232-6248
www.ajtr.org /ISSN:1943-8141/AJTR0099135

Original Article

Human induced pluripotent stem cell-derived mesenchymal stem cell therapy effectively reduced brain infarct volume and preserved neurological function in rat after acute intracranial hemorrhage

Kuan-Hung Chen[1*], Kun-Chen Lin[1], Christopher Glenn Wallace[2], Yi-Chen Li[3], Pei-Lin Shao[4], John Y Chiang[5], Pei-Hsun Sung[3], Hon-Kan Yip[3,4,6,7,8*]

[1]Department of Anesthesiology, Kaohsiung Chang Gung Memorial Hospital and Chang Gung University College of Medicine, Kaohsiung 83301, Taiwan; [2]Department of Plastic Surgery, University Hospital of South Manchester, Manchester, UK; [3]Division of Cardiology, Department of Internal Medicine, Kaohsiung Chang Gung Memorial Hospital and Chang Gung University College of Medicine, Kaohsiung 83301, Taiwan; [4]Department of Nursing, Asia University, Taichung 41354, Taiwan; [5]Department of Computer Science and Engineering, National Sun Yat-Sen University, Kaohsiung, Taiwan; [6]Institute for Translational Research in Biomedicine, Kaohsiung Chang Gung Memorial Hospital, Kaohsiung 83301, Taiwan; [7]Center for Shockwave Medicine and Tissue Engineering, Kaohsiung Chang Gung Memorial Hospital, Kaohsiung 83301, Taiwan; [8]Department of Medical Research, China Medical University Hospital, China Medical University, Taichung 40402, Taiwan. [*]Equal contributors.

Received July 1, 2019; Accepted August 29, 2019; Epub September 15, 2019; Published September 30, 2019

Abstract: We tested the hypothesis that human induced pluripotent stem cell-derived mesenchymal stem cell (iPSC-MSC) therapy could effectively reduce brain-infarct volume (BIV) and improve neurological function in rat after acute intracranial hemorrhage (ICH) induced by a weight-drop device. Adult-male SD rats (n=40) were equally divided into group 1 (sham-operated control), group 2 (ICH), group 3 (ICH + hyaluronic acid (HA)/intracranial injection at 3 h after ICH), group 4 [ICH + HA + iPSC-MSC (1.2×10^6 cells/intracranial injection at 3 h after ICH)] and euthanized by day 28 after ICH procedure. In vitro study showed that hemorrhagic-brain tissue augmented protein expressions of inflammation (HMGB1/MyD88/TLR-4/TLR-2/NF-κB/TNF-α/iNOS/IL-1β) in cultured neurons that were significantly inhibited by iPSC-MSC treatment (all P<0.001). By days 7 and 14 after ICH procedure, circulating inflammatory levels of TNF-α/IL-6/MPO expressed were lowest in group 1, highest in group 2 and significantly lower in group 4 than in group 3 (all P<0.0001). By day 14 after ICH procedure, neurological function and BIV expressed an opposite pattern, whereas protein expressions of inflammation (HMGB1/MyD88/TLR-4/TLR-2/NF-κB/I-kB/TNF-α/iNOS/IL-1β/MMP-9), oxidative stress (NOX-1/NOX-2/oxidized protein) and apoptosis (mitochondrial-Bax/cleaved-caspase-2/PARP) in brain exhibited an identical pattern to circulating inflammation among the four groups (all P<0.001). Microscopy demonstrated that the number of vascular remodeling and GFAP+/53BP1+/γ-H2AX+ cells displayed an identical pattern of inflammation, whereas the NeuN+ cells displayed an opposite pattern of inflammation among the four groups (all P<0.001). In conclusion, iPSC-MSC therapy markedly reduced BIV and preserved neurological function mainly by inhibiting inflammatory/oxidative-stress generation.

Keywords: Hemorrhagic stroke, iPSC-MSC, inflammation, oxidative stress

Introduction

Intracerebral hemorrhage (ICH) causes 10%-20% of all strokes, has a mortality rate of approximately 40%, and results in higher morbidity compared to other subtypes of cerebral stroke [1]. Expansion of the hematoma resulting in brain edema/swelling, compression of cerebral tissues with midline shift of the cerebral hemispheres, increased intracranial pressure, and brain stem herniation are the crucial contributors to morbidity and mortality in the acute stage. Although early surgical intervention can clear the expanding hematoma and ameliorate raised intracranial pressure, clinical outcomes following ICH have not significantly improved

over decades [2-5]. Accordingly, it is imperative that new, safe and efficacious treatments are sought.

Abundant reports have revealed that brain damage resulted from ischemia, ICH and necrosis would often upregulate damage-associated molecular pattern (DAMP)-inflammatory signaling, followed by neuroinflammation which is a key factor in instituting secondary brain cascades characterized by glial activation, peripheral inflammatory cell infiltration, and secretion of inflammatory mediators [6-12]. Sustained and excessive inflammation can exacerbate brain edema, damage the blood-brain barrier (BBB), lead to secondary neuronal injury, and generate increasing oxidative stress and neurological impairment through the secretion of pro-inflammatory mediators [6-11].

Plentiful data have shown that mesenchymal stem cell (MSC) therapy effectively improved ischemia-related organ dysfunction mainly through their anti-inflammatory, immunomodulatory and tissue regenerative properties [13-17]. Interestingly, MSC therapy reportedly led to regeneration of damaged neurons and improved long-term outcomes after hemorrhagic stroke [18-21].

Recently, the use of induced pluripotent stem cell derived mesenchymal stem cells (iPSC-MSC) has emerged as an innovative option for regenerative medicine [22, 23] and as a therapeutic possibility for various disease entities [24-26]. Additionally, we have recently demonstrated that iPSC-MSC therapy significantly protected kidney against ischemia-reperfusion injury in rat mainly through inhibiting inflammation and generation of oxidative stress as well as immunomodulation [27]. Two studies have demonstrated [28, 29] that transplantation of iPSC effectively protected neurological function in rat after ICH. However, a full investigation of the impact of iPSC-MSC on acute ICH has not been undertaken. Furthermore, engineered hyaluronic acid (HA) hydrogel-assisted stem cell transplantation has been shown by previous studies to promote stem cell differentiation and improve prognosis after acute ischemic stroke [30-32]. In the current study, we investigate the therapeutic potential of HA-assisted iPSC-MSC on acute ICH, focusing on its effects on brain infarct volume (BIV) and neurological outcome.

Materials and methods

Ethics

All animal procedures were approved by the Institute of Animal Care and Use Committee at Kaohsiung Chang Gung Memorial Hospital (Affidavit of Approval of Animal Use Protocol No. 2015093002) and performed in accordance with the Guide for the Care and Use of Laboratory Animals.

Animals were housed in an Association for Assessment and Accreditation of Laboratory Animal Care International (AAALAC; Frederick, MD, USA)-approved animal facility in our hospital with controlled temperature and light cycles (24°C and 12/12 light cycle).

Brain tissue extraction from healthy and ICH animals

The procedure and protocol have been described in our previous report [12]. Six animals were used for the ICH procedure. Animals were euthanized 6 hours after ICH induction. The brain was first aseptically removed from each animal by an expert technician including the ICH zone (i.e., cortex region). The brain tissue (100 mg) was extracted, homogenized in 1.0 mL PBS containing a protease inhibitor (539-134, Millipore) and vortexed. The crude extracts were pelleted by centrifugation (1380 RCF for 5 minutes at 4°C) and the supernatants used immediately for subsequent experiments. Protein assay dye (Bio-Rad, Hercules, California, USA) was used to quantify the brain extract concentration. Preparation of the brain tissue extracts in healthy rats was identical.

In vitro study to elucidate the underlying signaling pathway of iPSC-MSC treatment for protecting neuron from ICH-induced damage and preserving neurological function

To evaluate the effects of iPSC-MSC on reducing ICH-induced damage-associated molecular pattern (DAMP) inflammatory signaling, we used the following five groups of neuron cells: (1) neuron cells (i.e., 3.0×10^5 NeuC co-cultured with the reagent), (2) NeuC + normal brain tissue extracts (NB^{ET}) [i.e., neuron cells co-cultured with healthy brain tissue extracts (1.0 μg/mL) for 24 hours], (3) NeuC co-cultured with brain hemorrhagic tissue-derived extracts

(HB^{ET}) (1.0 μg/mL) for 24 hours, (4) NeuC + NB^{ET} (1.0 μg/mL)] at the bottom of a Transwell and iPSC-MSC (1×10^5 cells) in the upper part of the Transwell (i.e., 6-well Transwell, Millipore), and (5) NeuN + BH^{ET} (1.0 μg/mL)] at the bottom of a Transwell and iPSC-MSC (1×10^5 cells) in the upper part of the Transwell (Millipore). The total cell lysates were harvested for Western blotting.

Neuron cells (i.e., the cell line) were bought from the manufacturer [i.e., PC12 purchased from BCRC (Bioresource Collection and Research Center, Taiwan)]. Four additional rats were utilized for healthy brain tissue extracts and hemorrhagic brain tissue-derived extracts.

Animal grouping and study period

Pathogen-free, adult male (i.e., 10-12 week old) Sprague-Dawley rats (n = 40) weighing 325-350 g (Charles River Technology, BioLASCO, Taiwan) were randomly categorized into four groups: sham-operated control (SC) (i.e., group 1), ICH (group 2), ICH + hyaluronic acid (HA=40 μL) by intracranial injection 3 h after ICH (group 3), ICH + HA + iPSC-MSC (1.2×10^6 cells mix with 20 μL culture medium and 20 μL of HA) by direct intracranial injection 3 h after ICH) (group 4). All animals were euthanized by day 14 after ICH procedure.

The dosage of iPSC-MSCs in the present study was based on our previous studies [14, 16, 17]. Additionally, HA hydrogel was utilized in the present study to provide a scaffold for iPSC-MSC transplantation, differentiation and survival as well as brain tissue repair by iPSC-MSCs after ICH.

Four of the 10 animals in each group were utilized for assessment of the brain infarct area. The remainder (i.e., n=6 in each group) were utilized for molecular-cellular investigations.

ICH model using a weight-drop device in rat

Marmarou weight-drop model was used for the rat model of ICH as previously described [33-35]. Animals in the four groups were anesthetized by inhalational 2.0% isoflurane, placed supine on a warming pad at 37°C and then transferred to the weight-drop unit. A 1.5 cm long midline scalp incision was used to expose the skull in each group of animals. The left frontal region (3 mm posterior to the coronal suture, 1.5 mm lateral to the midline) was selected as the impact region. A 200-g weight-drop device (a metal ball with 6 mm diameter) was released and dropped onto the left frontal bone from a 2.5-cm height. With this method, an impact velocity of 6 m/second, and a dwell time of 150 msec (moderately severe injury) at an angle of 10° from the vertical plane produced an orthogonal impact with respect to the surface of the cortex. The scalp incision was then sutured. The sham group underwent the same procedure without the impact brain injury. The animals recovered from anaesthesia in a portable animal intensive care unit (ThermoCare®) for 24 hours.

Inclined plane test of hind limb muscle power and co-ordination

To assess the muscle power and co-ordination of the hind limbs of the rats, an inclined plane test was adopted as previously described with slight modifications [36]. During a five-day period of acclimatization in a temperature- and humidity-controlled room with 12-hour light-dark cycle and free access to water and standard animal chow, the rats were gently handled by laboratory personnel five times a day to let them accustom to human manipulation. In the following three days, the animals were placed on an inclined plane made of cardboard on which a horizontal friction strip provided a foothold for the animal's hind limbs as the inclination angle increased to prevent the animal from sliding down the slope. During the actual inclined plane test, each animal was placed on the inclined plane so that a secure foothold was established between the claws of its hind limbs and the friction strip. After confirmation of correct body position in the absence of anxious behavior and abnormally tense muscle tone of the animal, the inclination angle was slowly increased until the animal's hind limbs lost grasp of the friction strip and slid down the plane. The inclination angle was then recorded. After performing the experiment three times for each animal, the mean inclination angle was obtained by averaging the three recordings. The whole procedure was conducted by two independent technicians blinded to grouping of the animals.

Brain magnetic resonance imaging (MRI) examination

The procedure and protocol for brain magnetic resonance imaging (MRI) has been described

in our previous study [37]. MRI was assessed at days 2, 7 and 14 after ICH induction. Briefly, for MRI, rats were anesthetized by 3% inhalational isoflurane with room air and placed in an MRI-compatible holder (Biospec 94/20, Bruker, Ettingen, Germany). MRI data were collected using a Varian 9.4T animal scanner (Biospec 94/20, Bruker, Ettingen, Germany) with a rat surface array. The MRI protocol consisted of 40 T2-weighted images. Forty continuous slice locations were imaged with a field-of-view of 30 mm × 30 mm, an acquisition matrix dimension of 256 × 256 and slice thickness of 0.5 mm. The repetition time (TR) and echo time (TE) for each fast spin-echo volume were 4200 ms and 30 ms, respectively. Custom software, ImageJ (1.43i, NIH, USA), was used to process the region of interest (ROI). Planimetric measurements of images from MRI T2 were performed to calculate stroke volumes. Four of 10 animals in each group were randomly selected for brain MRI examination.

Immunofluorescent (IF) staining

The procedure and protocol for IF staining has been reported in our previous studies [14-17]. For IF staining, rehydrated paraffin sections were first treated with 3% H_2O_2 for 30 minutes and incubated with Immuno-Block reagent (BioSB, Santa Barbara, CA, USA) for 30 minutes at room temperature. Sections were then incubated with primary antibodies specifically against CD31 (1:100, Bio-Rad), von Willebrand factor (vWF) (1:200, Merck Millipore), 53BP1 (1:1000, Novus Biologicals), γ-H2AX (1:1000, Abcam), glial fibrillary acidic protein (GFAP) (1:500, Dako) and NeuN (1:100, Merck Millipore), while sections incubated with the use of irrelevant antibodies served as controls. Three sections of brain specimen from each rat were analyzed. For quantification, three random HPFs (200 × or 400 × for ICH and IF studies) were analyzed in each section. The mean number of positively-stained cells per HPF for each animal was then determined by summation of all numbers divided by 9.

Western blot analysis

The procedure and protocol for Western blot analysis have been reported by our previous studies [14-17]. Briefly, equal amounts (50 mg) of protein extracts were loaded and separated by SDS-PAGE using acrylamide gradients. After electrophoresis, the separated proteins were transferred electrophoretically to a polyvinylidene difluoride membrane (GE, UK). Nonspecific sites were blocked by incubation of the membrane in blocking buffer [5% nonfat dry milk in T-TBS (TBS containing 0.05% Tween 20)] overnight. The membranes were incubated with appropriate primary antibodies [cleaved caspase 3 (1:1000, Cell Signaling), cleaved poly (ADP-ribose) polymerase (PARP) (1:1000, Cell Signaling), mitochondrial Bax (1:1000, Abcam), nuclear factor (NF)-κB (1:1000, Abcam), tumor necrosis factor (TNF)-α (1:1000, Cell Signaling), interleukin (IL)-1b (1:1000, Cell Signaling), inducible nitric oxide synthase (iNOS) (1:250, Abcam), matrix metalloproteinase (MMP)-9 (1:1000, Abcam), NOX-1 (1:1500, Sigma), NOX-2 (1:750, Sigma), γ-H2AX (1:1000, Cell Signaling), high-mobility group protein 1 (HMGB1) (1:1000, Cell Signaling), I-κB (1:1000, Abcam), myeloid differentiation primary response 88 (MYD88) (1:1000, Abcam), toll-like receptor (TLR)-2 (1:1000, Abcam), TLR-4 (1:1000, Abcam) and Actin (1:1000, Millipore)] for 1 hour at room temperature. Horseradish peroxidase-conjugated anti-rabbit immunoglobulin IgG (1:2000, Cell Signaling, Danvers, MA, USA) was used as a secondary antibody for one-hour incubation at room temperature. The washing procedure was repeated eight times within one hour. Immunoreactive bands were identified by enhanced chemiluminescence (ECL; Amersham Biosciences, Amersham, UK) and exposed to Biomax L film (Kodak, Rochester, NY, USA). For quantification, ECL signals were digitized using Labwork software (UVP, Waltham, MA, USA).

Assessment of oxidative stress

The procedure and protocol for assessing protein expression of oxidative stress were reported by our previous studies [14-17]. The Oxyblot Oxidized Protein Detection Kit was purchased from Chemicon, Billerica, MA, USA (S7150). DNPH derivatization was carried out on 6 μg of protein for 15 minutes according to the manufacturer's instructions. One-dimensional electrophoresis was carried out on 12% SDS/polyacrylamide gel after DNPH derivatization. Proteins were transferred to nitrocellulose membranes which were then incubated in the primary antibody solution (anti-DNP 1:150) for 2 hours, followed by incubation in secondary antibody solution (1:300) for 1 hour at room tem-

perature. Immunoreactive bands were visualized by enhanced chemiluminescence (ECL; Amersham Biosciences, Amersham, UK) which was then exposed to Biomax L film (Kodak, Rochester, NY, USA). For quantification, ECL signals were digitized using Labwork software (UVP, Waltham, MA, USA). For Oxyblot protein analysis, a standard control was loaded on each gel.

Measurement of arterial muscularization and dilatation in brain infarct zone

Immunohistochemical staining of α-smooth muscle actin (Sigma) was performed to identify arterial muscularization as previously described [38]. Briefly, three sections of brain specimen from each rat were used and three randomly selected high-power fields (HPFs) (400 ×) were analyzed in each section. The mean number per HPF for each animal was then determined by summation of all numbers at each level divided by 9. Finally, the mean number of vessels in the brain infarct zone was obtained by averaging the mean number of vessels at each level. Muscularization of the arterial medial layer in brain parenchyma was defined as a mean thickness of vessel wall greater than 50% of the lumen diameter in a vessel of diameter >30 μm, or if the medial layer increased more than 50% of the original medial layer. Additionally, vessel dilatation was defined when the vessel diameter in the brain infarct zone was greater than three times that of the normal vessel in healthy animals by HPFs.

Statistical analysis

Quantitative data were expressed as means ± SD. Statistical analysis was adequately performed by ANOVA followed by Bonferroni multiple comparison post hoc test. SAS statistical software for Windows version 8.2 (SAS institute, Cary, NC) was utilized. A probability value <0.05 was considered statistically significant.

Results

*Time courses of brain MRI findings for identification of hematoma volume (**Figure 1**)*

By days 2, 7 and 14 after ICH induction, brain hematoma volume was significantly lower in SC (i.e., group 1) than in the other groups, significantly higher in groups ICH (group 2) and ICH-HA (group 3) than in ICH-HA-iPSC-MSC (group 4), but it showed no difference between groups 2 and 3.

*Time courses of neurological function and brain hematoma area (**Figure 2**)*

By days 1 and 7 after acute ICH procedure, the inclined plane test for determining limb motor function demonstrated that this parameter was significantly higher in group 1 than in the other groups but not different among groups 2 to 4. Additionally, by day 14 after ICH procedure, this parameter was significantly higher in group 1 than in other groups, significantly higher in group 4 than in groups 2 and 3, but not different between the latter two groups.

By day 14, the brain hematoma area (i.e., identified by H.E. staining and calculated by summations of five whole brain cross sections in each animal) showed an identical pattern of brain infarct volume by MRI among the four groups. Importantly, no tumorigenesis was evident on brain MRI or histopathology (by H.E. stain) in iPSC-MSC treated animals.

*iPSC-MSC downregulated the DAMP-signaling inflammatory pathway in neurons (**Figure 3**)*

In vitro study demonstrated that the protein expression of HMGB1, an indicator of DAMP, was significantly increased NeuN + BH^{ET} than in other groups, significantly higher in NeuN + BH^{ET} + iPSC-MSC than in NeuN, NeuN + NB^{ET} and NeuN + NB^{ET} + iPSC-MSC, but they showed no difference among the latter three groups. Additionally, the protein expressions of TLR-2 and TLR-4, two indicators of inflammation that indicate the down-stream signaling pathway of HMGB1, exhibited an identical pattern to HMGB1 among the five groups. Furthermore, the protein expressions of MyD88 and I-κB/NF-κB, three inflammatory biomarkers that act in the down-stream signaling pathway of TLR-2/TLR-4, also exhibited an identical pattern to HMGB1 among the five groups. Finally, the protein expressions of TNF-α, iNOS, IL-1β and MMP-9, four indicators of inflammation and the translated products (by the nuclear system) resultant from DAMP stimulation, displayed an identical pattern to NF-κB among the five groups.

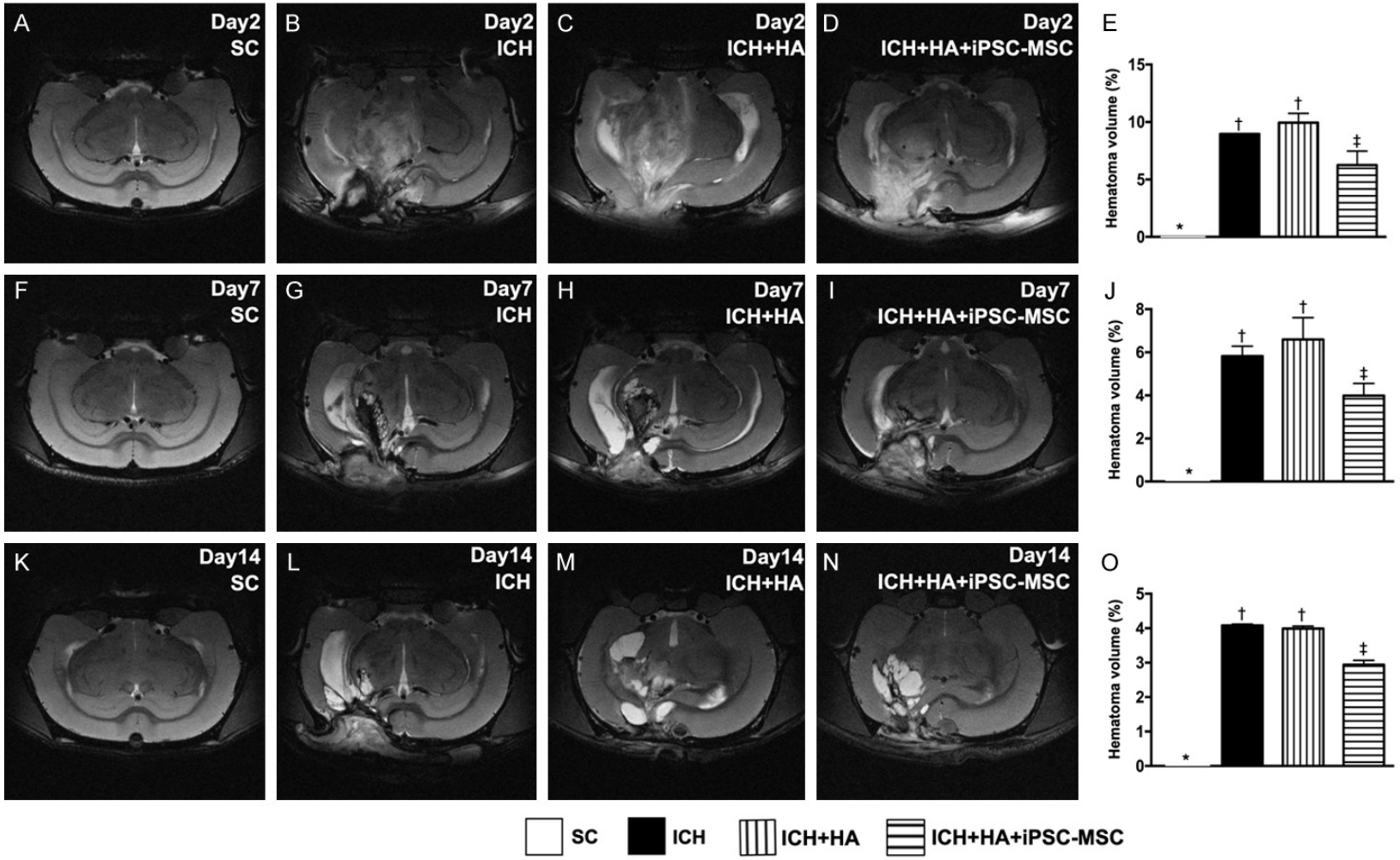

Figure 1. Time courses of brain magnetic resonance imaging (MRI). A-D. Illustrating brain MRI by day 2 after ICH induction (white color). E. Analysis of brain hematoma volume, * vs. other groups with different symbols (†, ‡), P<0.0001. F-I. Illustrating brain MRI by day 7 after acute ICH induction (white color). J. Analysis of brain hematoma volume, * vs. other groups with different symbols (†, ‡), P<0.0001. K-N. Illustrating brain MRI by day 14 after acute ICH induction (white color). O. Analysis of brain hematoma volume, * vs. other groups with different symbols (†, ‡), P<0.0001. All statistical analyses were performed by one-way ANOVA, followed by Bonferroni multiple comparison post hoc test (n=4 for each group). Symbols (*, †, ‡) indicate significance (at 0.05 level). SC = sham control; HA = hyaluronic acid; ICH = intracranial hemorrhage; iPSC-MSC = human induced pluripotent stem cell-derived mesenchymal stem cell.

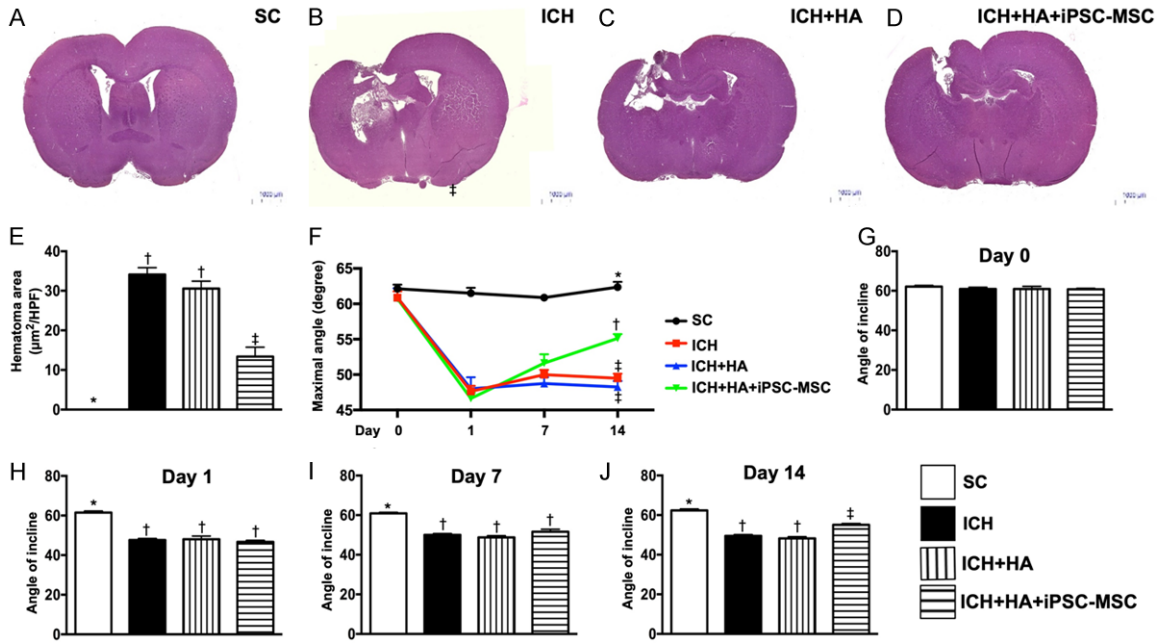

Figure 2. Brain hematoma area (BHA) at day 14 and serial changes of inclined plane test for assessment of limb motor function after ICH. A-D. Illustrating the H.E stain (100 ×) of whole brain cross section for identification of BHA (the yellow dotted line indicates the boundary of BHA) by day 3 after ICH procedure (n=4). E. Statistical analysis of summated (five cross section in each animal) BHA, * vs. other groups with different symbols (†, ‡), P<0.0001. F. Illustrating the inclined plane test for determining limb motor function among days 0, 7 and 14 after acute ICH procedure. G. Statistical analysis by day 0, P=1. H. Statistical analysis by day 1, * vs. †P<0.0001. I. Statistical analysis by day 7, * vs. †P<0.0001. J. Statistical analysis by day 14, * vs. other groups with different symbols (†, ‡), P<0.001. All statistical analyses were performed by one-way ANOVA, followed by Bonferroni multiple comparison post hoc test (n=10 for inclined plane test in each group). Symbols (*, †, ‡) indicate significance (at 0.05 level). SC = sham control; ICH = intracranial hemorrhage; HA = hyaluronic acid; iPSC-MSC = human induced pluripotent stem cell-derived mesenchymal stem cell.

*Serial changes of circulatory levels of inflammatory biomarkers (**Figure 4**)*

By day 0, circulating levels of TNF-α, IL-6 and myeloperoxidase (MPO), three indicators of inflammation, did not differ among the four groups. However, by days 1, 3, 7, and 14 after ICH induction, these parameters were highest in group 2, lowest in group 1 and significantly lower in group 4 than in group 3.

*Protein expressions of DAMP-inflammatory signaling pathway in brain tissue by day 14 after ICH procedure (**Figure 5**)*

As expected, protein expressions of HMGB1, TLR-2, TLR-4, MyD88, I-κB, NF-κB, six indicators of inflammation, were significantly lowest in group 1, highest in group 2 and significantly lower in group 4 than in group 3. Additionally, protein expressions of IL-1β, MMP-9, TNF-α, iNOS, another four indicators of inflammation, displayed an identical pattern to HMGB1 among the four groups.

*The protein expressions of oxidative stress and apoptosis in brain tissue, and the numbers of arterial muscularization/dilatation, and endothelial cell markers in brain hematoma zone by day 14 after ICH procedure (**Figure 6**)*

The protein expressions of mitochondrial Bax, cleaved caspase 3 and cleaved PARP, three indices of apoptosis, were highest in group 2, lowest in group 1, and significantly higher in group 3 than in group 4. Additionally, the protein expressions of NOX-1, NOX-2 and oxidized protein, three indicators of oxidative stress, revealed an identical pattern to apoptosis.

The number of arterial muscularizations, an indicator of arterial remodeling, was significantly higher in group 2 than in other groups, significantly higher in group 3 than in groups 1 and 4,

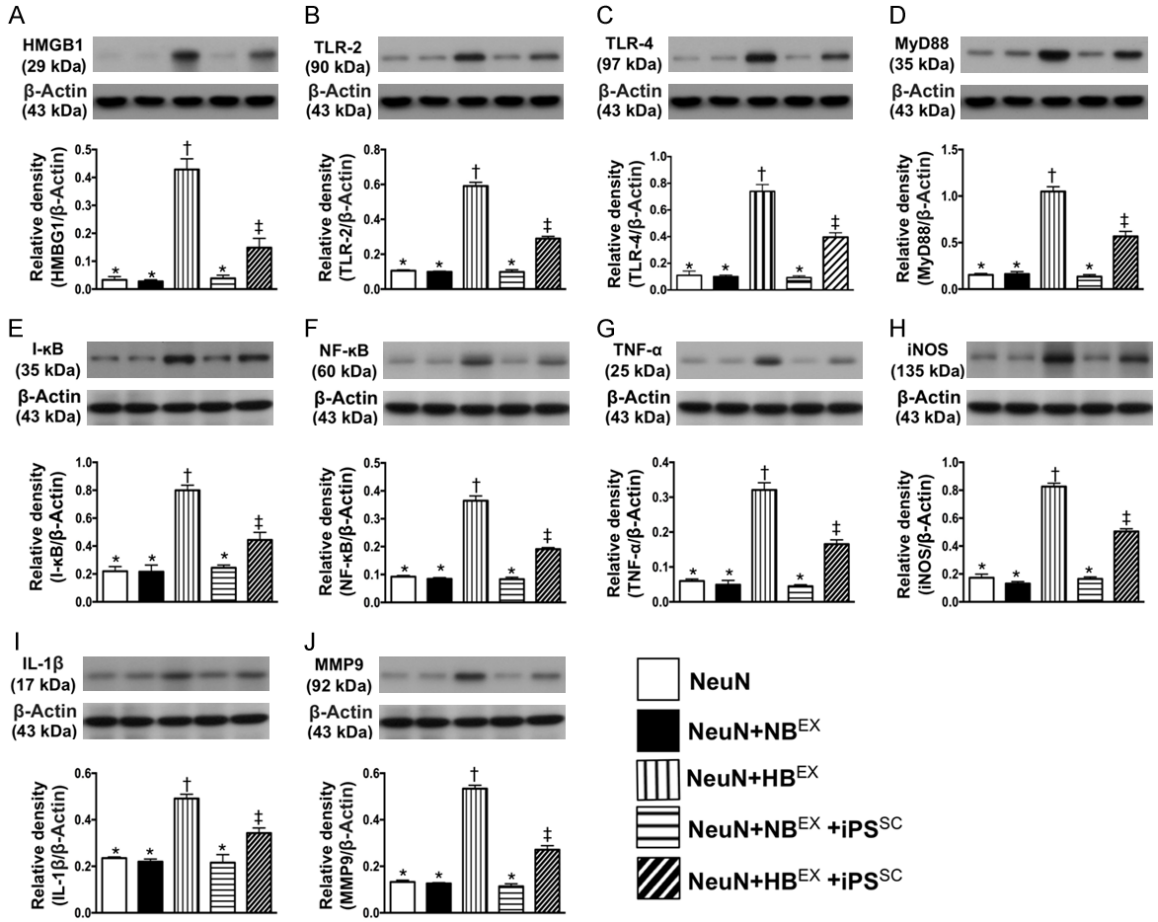

Figure 3. iPSC-MSC suppressed the DAMP-signaling inflammatory pathway in neuron cell line. A. Protein expression of high-mobility group protein 1 (HMGB1), * vs. other groups with different symbols (†, ‡), P<0.0001. B. Protein expression of toll-like receptor (TLR)-2, * vs. other groups with different symbols (†, ‡), P<0.0001. C. Protein expression of TLR-4, * vs. other groups with different symbols (†, ‡), P<0.0001. D. Protein expressions of myeloid differentiation primary response 88 (MyD88), * vs. other groups with different symbols (†, ‡), P<0.0001. E. Protein expression of I-κB, * vs. other groups with different symbols (†, ‡), P<0.0001. F. Protein expression of nuclear factor (NF)-κB, * vs. other groups with different symbols (†, ‡), P<0.0001. G. Protein expression of tumor necrosis factor (TNF-α), * vs. other groups with different symbols (†, ‡), P<0.0001. H. Protein expression of inducible nitric oxide synthase (iNOS), * vs. other groups with different symbols (†, ‡), P<0.0001. I. Protein expression of interleukin (IL)-1β, * vs. other groups with different symbols (†, ‡), P<0.001. J. Protein expression of matrix metalloproteinase (MMP)-9, * vs. other groups with different symbols (†, ‡), P<0.0001. All statistical analyses were performed by one-way ANOVA, followed by Bonferroni multiple comparison post hoc test (n=4 for each group). Symbols (*, †, ‡) indicate significance (at 0.05 level). NeuN = neuron cell line treated by reagent; NB^{EX} = indicated NeuN treated by normal brain tissue extracts (NB^{EX}); HB^{EX} = hemorrhagic brain tissue-derived extracts; iPSC-MSC = induced pluripotent stem cell-derived mesenchymal stem cell.

and significantly higher in group 4 than in group 1. Additionally, the number of arterial dilatations (relative to the reference of arterial diameter of the SC), another indicator of arterial remodeling, exhibited an identical pattern to arterial muscularizations among the four groups.

Furthermore, IF microscopy demonstrated that the number of positively stained CD31/vWF cells in vessels, an endothelial cell surface marker, also exhibited an identical pattern to arterial dilatations, suggesting that this finding correlated with the result of arterial dilatation.

*Expressions of glial cells and NeuN cells in brain tissue by day 14 after ICH procedure (**Figure 7**)*

The cellular expression of positively stained GFAP, an indicator of inflammation in brain parenchyma, was highest in group 2, lowest in

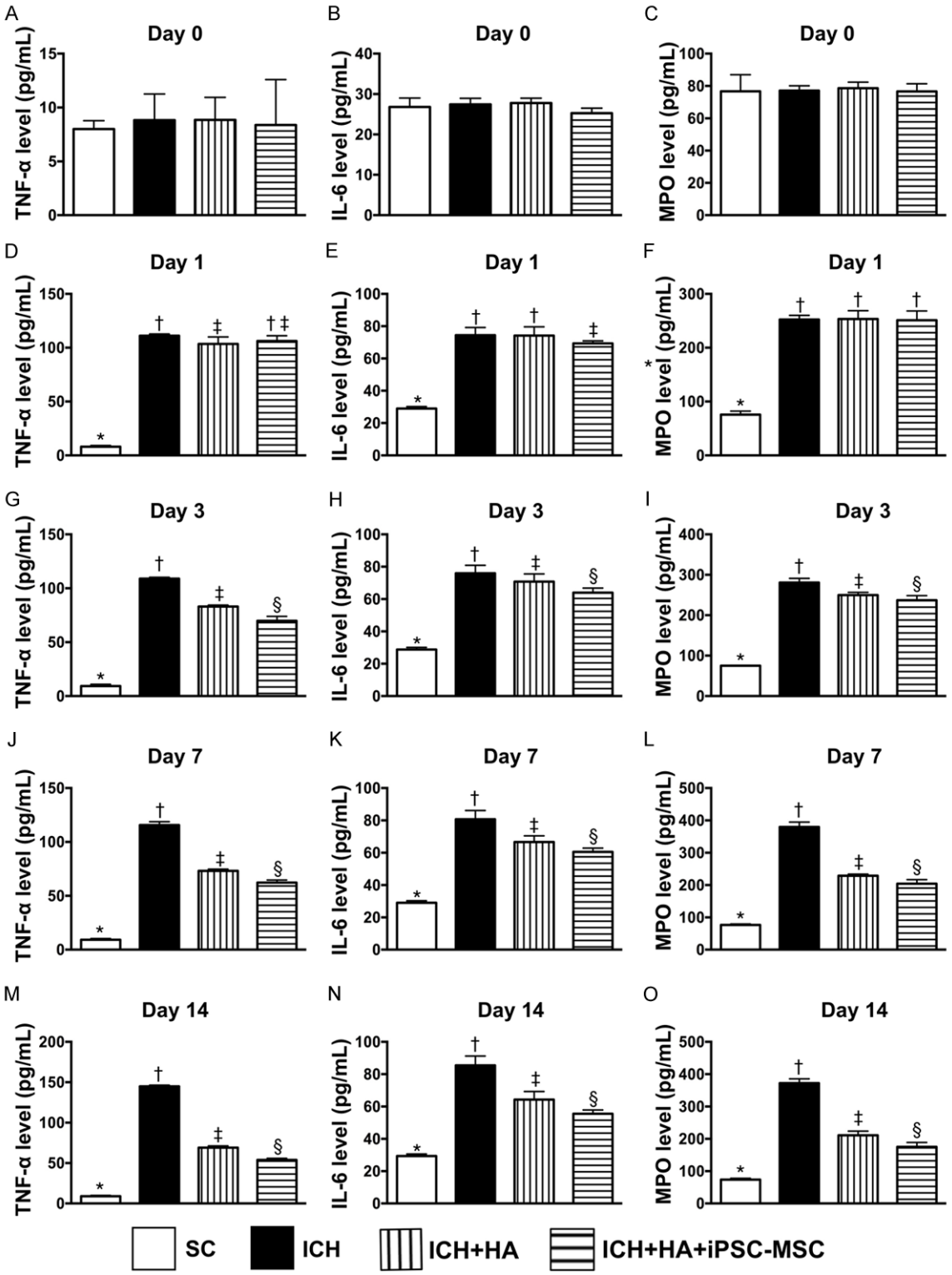

Figure 4. Time courses of circulatory levels of inflammatory biomarkers prior to and after acute ICH. A. By day 0, analytical result of circulating level of tumor necrosis factor (TNF)-α, P>0.5. B. By day 0, analytical result of circulating level of interleukin (IL)-6, P>0.5. C. By day 0, analytical result of circulating level of myeloperoxidase (MPO), P>0.5. D. By day 1, analytical result of circulating level of TNF-α, * vs. other groups with different symbols (†, ‡), P<0.0001. E. By day 1, analytical result of circulating level of IL-6, * vs. other groups with different symbols (†, ‡), P<0.0001. F. By day 1, analytical result of circulating level of MPO, * vs. †, P<0.0001. G. By day 3, analytical result of circulating level of TNF-α, * vs. other groups with different symbols (†, ‡, §), P<0.0001. H. By day 3, analytical

result of circulating level of IL-6, * vs. other groups with different symbols (†, ‡, §), P<0.0001. I. By day 3, analytical result of circulating level of MPO, * vs. other groups with different symbols (†, ‡, §), P<0.0001. J. By day 7, analytical result of circulating level of TNF-α, * vs. other groups with different symbols (†, ‡, §), P<0.0001. K. By day 7, analytical result of circulating level of IL-6, * vs. other groups with different symbols (†, ‡, §), P<0.0001. L. By day 7, analytical result of circulating level of MPO, * vs. other groups with different symbols (†, ‡, §), P<0.0001. M. By day 14, analytical result of circulating level of TNF-α, * vs. other groups with different symbols (†, ‡, §), P<0.0001. N. By day 14, analytical result of circulating level of IL-6, * vs. other groups with different symbols (†, ‡, §), P<0.0001. O. By day 14, analytical result of circulating level of MPO, * vs. other groups with different symbols (†, ‡, §), P<0.0001. All statistical analyses were performed by one-way ANOVA, followed by Bonferroni multiple comparison post hoc test (n = 6 for each group). Symbols (*, †, ‡, §) indicate significance (at 0.05 level). SC = sham-operated control; ICH = intracranial hemorrhage; HA = hyaluronic acid; ICH = intracranial hemorrhage; iPSC-MSC = induced pluripotent stem cell-derived mesenchymal stem cell.

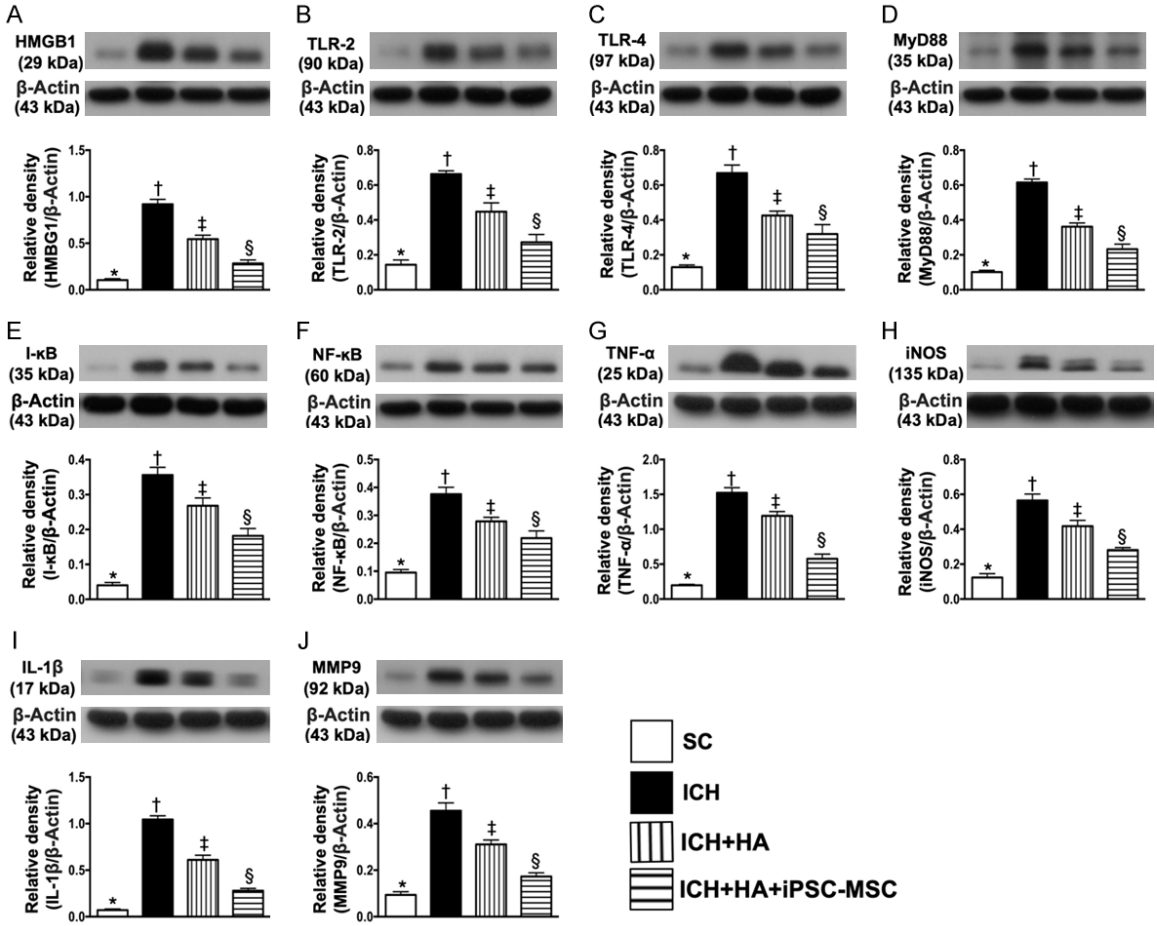

Figure 5. Protein expressions of DAMP-inflammatory signaling pathway in brain tissue by day 14 after ICH procedure. A. Protein expression of high-mobility group protein 1 (HMGB1), * vs. other groups with different symbols (†, ‡, §), P<0.0001. B. Protein expression of toll-like receptor (TLR)-2, * vs. other groups with different symbols (†, ‡, §), P<0.0001. C. Protein expression of TLR-4, * vs. other groups with different symbols (†, ‡, §), P<0.0001. D. Protein expressions of myeloid differentiation primary response 88 (MyD88), * vs. other groups with different symbols (†, ‡, §), P<0.0001. E. Protein expression of I-κB, * vs. other groups with different symbols (†, ‡, §), P<0.0001. F. Protein expression of nuclear factor (NF)-κB, * vs. other groups with different symbols (†, ‡, §), P<0.0001. G. Protein expression of tumor necrosis factor (TNF-α), * vs. other groups with different symbols (†, ‡, §), P<0.0001. H. Protein expression of inducible nitric oxide synthase (iNOS), * vs. other groups with different symbols (†, ‡, §), P<0.0001. I. Protein expression of interleukin (IL)-1β, * vs. other groups with different symbols (†, ‡, §), P<0.0001. J. Protein expression of matrix metalloproteinase (MMP)-9, * vs. other groups with different symbols (†, ‡, §), P<0.0001. All statistical analyses were performed by one-way ANOVA, followed by Bonferroni multiple comparison post hoc test (n=6 for each group). Symbols (*, †, ‡, §) indicate significance (at 0.05 level). SC = sham-operated control; ICH = intracranial hemorrhage; HA = hyaluronic acid; iPSC-MSC = induced pluripotent stem cell-derived mesenchymal stem cell.

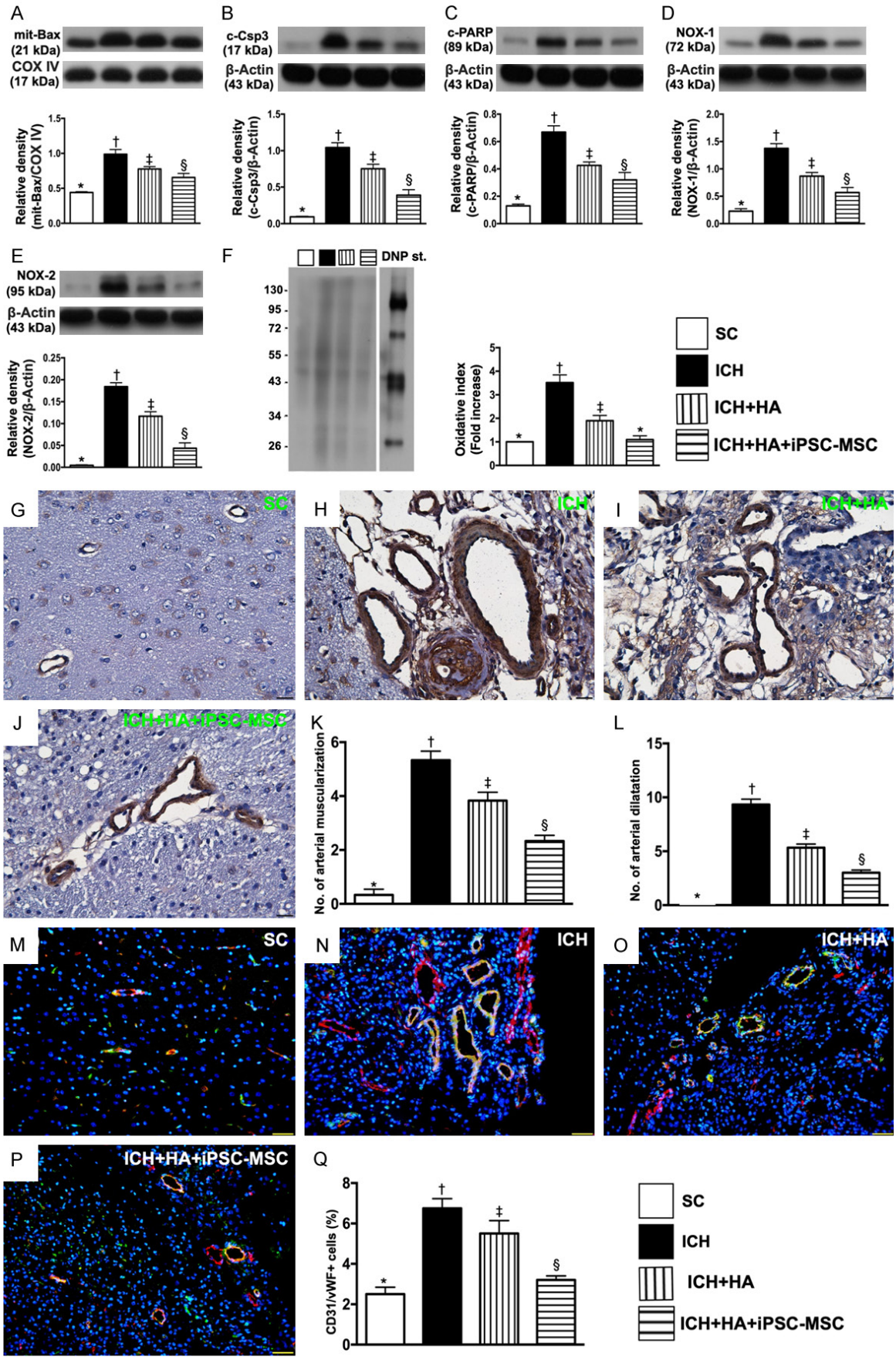
A
mit-Bax (21 kDa)
COX IV (17 kDa)
Relative density (mit-Bax/COX IV)
B
c-Csp3 (17 kDa)
β-Actin (43 kDa)
Relative density (c-Csp3/β-Actin)
C
c-PARP (89 kDa)
β-Actin (43 kDa)
Relative density (c-PARP/β-Actin)
D
NOX-1 (72 kDa)
β-Actin (43 kDa)
Relative density (NOX-1/β-Actin)
E
NOX-2 (95 kDa)
β-Actin (43 kDa)
Relative density (NOX-2/β-Actin)
F
DNP st.
130
95
72
55
43
34
26
Oxidative index (Fold increase)
SC
ICH
ICH+HA
ICH+HA+iPSC-MSC
G
SC
H
ICH
I
ICH+HA
J
ICH+HA+iPSC-MSC
K
No. of arterial muscularization
L
No. of arterial dilatation
M
SC
N
ICH
O
ICH+HA
P
ICH+HA+iPSC-MSC
Q
CD31/vWF+ cells (%)
SC
ICH
ICH+HA
ICH+HA+iPSC-MSC

Figure 6. The protein expressions of oxidative-stress and apoptotic biomarkers in brain tissue, and the numbers of arterial muscularization/dilatation and endothelial cell markers in brain hematoma zone by day 14 after ICH procedure. A. The protein expressions of mitochondrial (Mito) Bax, * vs. other groups with different symbols (†, ‡, §), P<0.0001. B. Protein expression of cleaved caspase 3 (c-Csp-3), * vs. other groups with different symbols (†, ‡, §), P<0.0001. C. Protein expression of cleaved Poly (ADP-ribose) polymerase (c-PARP), * vs. other groups with different symbols (†, ‡, §), P<0.0001. D. Protein expression of NOX-1, * vs. other groups with different symbols (†, ‡, §), P<0.0001. E. Protein expression of NOX-2, * vs. other groups with different symbols (†, ‡, §), P<0.0001. F. Oxidized protein expression, * vs. other groups with different symbols (†, ‡, §), P<0.0001. (Note: left and right lanes shown on the upper panel represent protein molecular weight marker and control oxidized molecular protein standard, respectively). M.W = molecular weight; DNP = 1-3 dinitrophenylhydrazone. G-J. Illustrating microscopic finding (400 ×) of α-smooth muscle actin (α-SMA) staining for identification of arterial muscularization (red arrows) and arterial dilatation (yellow arrows). K. Analytical result of number of arterial muscularizations, * vs. other groups with different symbols (†, ‡, §), P<0.0001. L. Analytical result of number of arterial dilatations, * vs. other groups with different symbols (†, ‡, §), P<0.0001. M-P. Illustrating immunofluorescent (IF) microscopy (400 ×) for identification of positively stained CD31/von Willebrand factor (CD31/vWF+) cells in vessels, i.e., double stain of green-yellow color. Q. Analytical result of number of CD31/vWF+ cells, * vs. other groups with different symbols (†, ‡, §), P<0.001. Scale bars in the right lower corner represent 20 μm. All statistical analyses were performed by one-way ANOVA, followed by Bonferroni multiple comparison post hoc test (n=6 for each group). Symbols (*, †, ‡, §) indicate significance (at 0.05 level). SC = sham-operated control; ICH = intracranial hemorrhage; HA = hyaluronic acid; iPSC-MSC = induced pluripotent stem cell-derived mesenchymal stem cell.

group 1 and significantly lower in group 4 than in group 3. Additionally, the cellular expression of positively stained NeuN, an indicator of integrity of neurons, displayed an opposite pattern to GFAP+ cells among the four groups.

*Cellular expressions of DNA-damaged biomarkers by day 14 after ICH procedure (**Figure 8**)*

The cellular expression of positively stained γ-H2AX, an indicator of single-strand DNA-damaged biomarker, was highest in group 2, lowest in group 1, and significantly lower in group 4 than in group 3. Additionally, the cellular expression of positively stained 53BP1, an indicator of double-stranded DNA, displayed an identical pattern to γ-H2AX among the four groups.

Discussion

This study investigated the therapeutic impact of human iPSC-MSC on ICH in rat and yielded several striking implications. First, no immune rejection or tumorigenesis was identified in this preclinical ICH study, suggesting that xenogeneic MSC therapy could be safe and has immune privilege. Second, brain infarct volume/area was remarkably reduced and neurological function was significantly improved in the current study, highlighting that this regimen may be a therapeutic option for ICH patients who prove refractory to conventional therapy.

Although preclinical studies [28, 29] have shown that iPSC significantly preserved neurological status in the setting of ICH, the issue of immune rejection has not previously been adequately addressed. Furthermore, the therapeutic impact of iPSC-MSC on ICH remains unknown. The most important finding in the present study was that, compared with ICH only animals, brain infarct volume (measured by brain MRI) and brain infarct area (measured by histopathology) were substantially reduced in ICH animals after receiving iPSC-MSC therapy. Our findings, in addition to strengthening those of previous limited studies [28, 29], could explain why neurological function was better preserved in ICH animals with, than in ICH animals without, iPSC-MSC treatment. Of importance, neither brain MRI nor histopathology could identify tumorigenesis. Intriguingly, our recent study [16] showed that xenogeneic human umbilical cord-derived mesenchymal stem cell therapy did not cause immune rejection, but also protected the lung from acute respiratory distress syndrome complicated by sepsis in rat. In this way, our present findings, in addition to being comparable to those of our recent report [16], highlight that iPSC-MSC therapy could be considered as a last resort option for severe ICH patients who are refractory to current therapy.

An essential finding in the present study was that, as compared with SC group, the molecular-cellular levels of oxidative-stress, apoptosis, GFAP, inflammatory and DNA-damaged biomarkers were remarkably increased in ICH animals. However, these molecular-cellular perturbations were markedly suppressed in ICH ani-

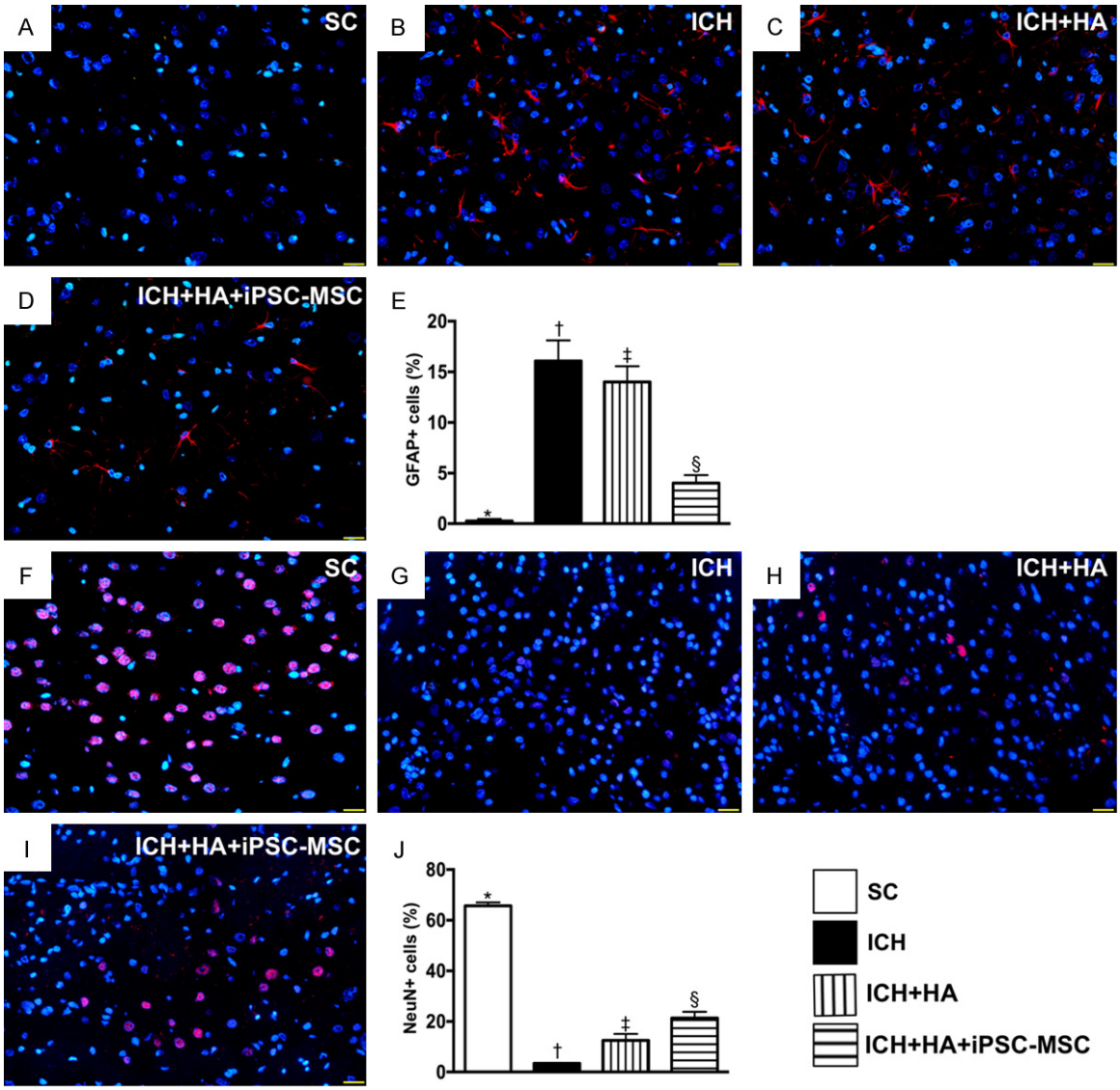

Figure 7. Expressions of glial cells and NeuN cells in brain tissue by day 14 after ICH procedure. A-D. Illustrating immunofluorescent (IF) microscopy (400 ×) for identification of glial fibrillary acid protein (GFAP)+ cells (red color). E. Analytic result of number of GFAP+ cells, * vs. other groups with different symbols (†, ‡, §), P<0.0001. F-I. Illustrating IF microscopy (400 ×) for identification of NeuN+ cells (pink color). J. Analytic result of number of GFAP+ cells, * vs. other groups with different symbols (†, ‡, §), P<0.0001. Scale bars in right lower corner represent 20 μm. All statistical analyses were performed by one-way ANOVA, followed by Bonferroni multiple comparison post hoc test (n=6 for each group). Symbols (*, †, ‡, §) indicate significance (at 0.05 level). SC = sham-operated control; ICH = intracranial hemorrhage; HA = hyaluronic acid; iPSC-MSC = induced pluripotent stem cell-derived mesenchymal stem cell.

mals by HA treatment and further markedly suppressed by HA + iPSC-MSC. Interestingly, previous studies have revealed that HA possesses anti-inflammatory properties and also acts as a scaffold for stem cell transplantation, improving prognosis after acute ischemic stroke [30-32]. In this way, our findings are comparable those of previous studies [30-32]. Of further interest in the present study was that arterial remodeling (i.e., muscularization and vessel dilatation) was markedly increased in ICH animals compared to SC, inhibited by HA, and further inhibited by HA + iPSC-MSC treatment. This finding suggests that HA acted as a scaffold to occupy the infarcted empty space, resulting in less arterial remodeling in the infarct zone.

The underlying mechanisms of stem cell therapy for improving ischemia-related organ dys-

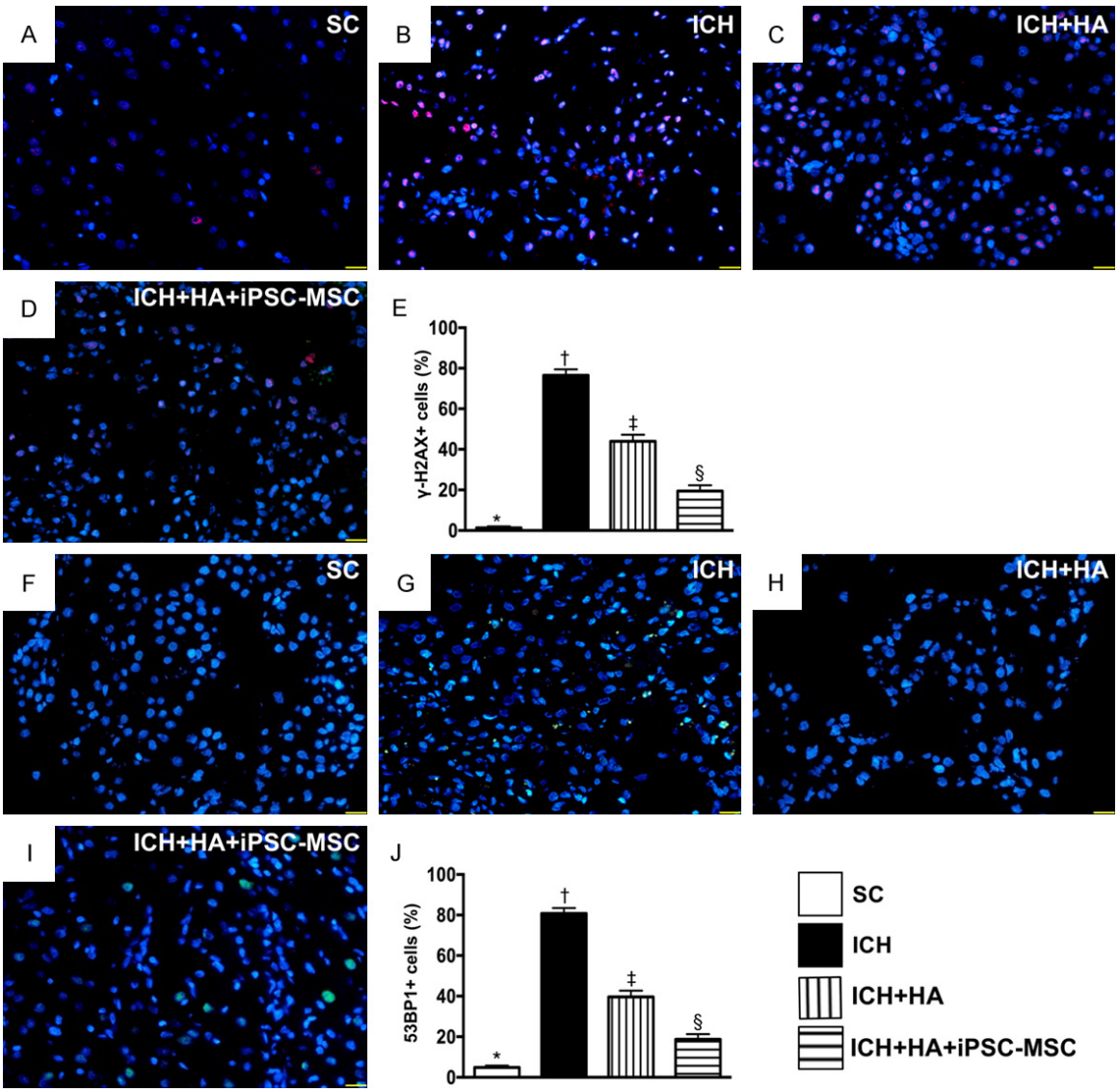

Figure 8. Cellular expressions of DNA-damaged biomarkers by day 14 after ICH procedure. A-D. Illustrating immunofluorescent (IF) microscopy (400 ×) for identification of positively-stained γ-H2AX cells (pink color). E. Analytic result of number of γ-H2AX+ cells, * vs. other groups with different symbols (†, ‡, §), P<0.0001. F-I. Illustrating IF microscopy (400 ×) for identification of positively-stained 53BP1 cells (green color). J. Analytic result of number of 53BP1+ cells, * vs. other groups with different symbols (†, ‡, §), P<0.0001. Scale bars in right lower corner represent 20 μm. All statistical analyses were performed by one-way ANOVA, followed by Bonferroni multiple comparison post hoc test (n=6 for each group). Symbols (*, †, ‡, §) indicate significance (at 0.05 level). SC = sham-operated control; ICH = intracranial hemorrhage; HA = hyaluronic acid; iPSC-MSC = induced pluripotent stem cell-derived mesenchymal stem cell.

function have been keenly investigated by previous studies [39, 40]; however, the exact mechanisms remain controversial. Intriguingly, DAMPs have been established to play an essential role that elicits the inflammatory reaction in response to tissue damage [41, 42]. DAMPs include endogenous intracellular molecules liberated by activated or by necrotic cells and extracellular matrices [42]. DAMPs commence signaling cascades that activate TLRs and MyD88, and further activate the downstream signaling of I-κB, nuclear factor-κB and interferon regulatory factors for transcription of interferon gene [42-44]. These factors stimulate the production of proinflammatory cytokines in damaged organs [42-46] which, in turn, further damage the organs and worsen their functions. A principal finding of our in vitro study

was that the protein expressions of HMGB1 (an indicator of DAMPs), TLR-2/TLR-4 and MyD88 were significantly increased in the neuron cell line-co-cultured with brain hemorrhagic tissue-derived extracts. Interestingly, when we also looked at the downstream signaling of MyD88, we found that the protein expressions of I-κB, NF-κB, TNF-α, IL-β and iNOS were also significantly increased in the neuron cell line with the same stimulating condition. However, these inflammatory molecular perturbations were significantly suppressed by iPSC-MSC released components. A distinctive finding in the in vivo study was that the DAMP signaling pathway also existed identically in the damaged brain tissues and were also ameliorated by HA + iPSC-MSC treatment. Accordingly, the findings of our in vitro and in vivo studies were consistent and provided novel explanations for the underlying mechanism of iPSC-MSC therapy when protecting brain tissue/neurons (i.e., NeuN cells) against ICH-induced injury.

Study limitations

This study has limitations. First, although short-term outcomes were promising, the long-term outcome of iPSC-MSC therapy in the setting of ICH remains uncertain due to the fact that the study period was relatively short (14 days). Second, although extensive work has been done in the present study, the underlying mechanisms of iPSC-MSC therapy for improving prognosis in rodent after ICH remain uncertain.

In conclusion, the results of the present study demonstrated that HA-scaffold-supported iPSC-MSC therapy reduced brain infarct volume and improved prognosis in rat after ICH mainly by inhibiting the DAMPs-signaling pathway.

Acknowledgements

This study was supported by a program grant from Chang Gung Memorial Hospital, Chang Gung University (Grant number: CMRPG8-E1361).

Disclosure of conflict of interest

None.

Address correspondence to: Kuan-Hung Chen, Department of Anesthesiology, Kaohsiung Chang Gung Memorial Hospital and Chang Gung University College of Medicine, 123 Dapi Road, Niaosung Dist., Kaohsiung 83301, Taiwan. Tel: +886-7-7317123; Fax: +886-7-7322402; E-mail: amigofx35@gmail.com; Hon-Kan Yip, Division of Cardiology, Department of Internal Medicine, Kaohsiung Chang Gung Memorial Hospital and Chang Gung University College of Medicine, 123 Dapi Road, Niaosung Dist., Kaohsiung 83301, Taiwan. Tel: +886-7-7317123; Fax: +886-7-7322402; E-mail: han.gung@msa.hinet.net

References

[1] van Asch CJ, Luitse MJ, Rinkel GJ, van der Tweel I, Algra A, Klijn CJ. Incidence, case fatality, and functional outcome of intracerebral haemorrhage over time, according to age, sex, and ethnic origin: a systematic review and meta-analysis. Lancet Neurol 2010; 9: 167-176.

[2] Morgenstern LB, Frankowski RF, Shedden P, Pasteur W, Grotta JC. Surgical treatment for intracerebral hemorrhage (STICH): a single-center, randomized clinical trial. Neurology 1998; 51: 1359-1363.

[3] NINDS ICH Workshop Participants. Priorities for clinical research in intracerebral hemorrhage: report from a National Institute of Neurological Disorders and Stroke workshop. Stroke 2005; 36: e23-41.

[4] Zhu J, Xiao Y, Li Z, Han F, Xiao T, Zhang Z, Geng F. Efficacy of surgery combined with autologous bone marrow stromal cell transplantation for treatment of intracerebral hemorrhage. Stem Cells Int 2015; 2015: 318269.

[5] Zuccarello M, Brott T, Derex L, Kothari R, Sauerbeck L, Tew J, Van Loveren H, Yeh HS, Tomsick T, Pancioli A, Khoury J, Broderick J. Early surgical treatment for supratentorial intracerebral hemorrhage: a randomized feasibility study. Stroke 1999; 30: 1833-1839.

[6] Chen X, Wu S, Chen C, Xie B, Fang Z, Hu W, Chen J, Fu H, He H. Omega-3 polyunsaturated fatty acid supplementation attenuates microglial-induced inflammation by inhibiting the HMGB1/TLR4/NF-kappaB pathway following experimental traumatic brain injury. J Neuroinflammation 2017; 14: 143.

[7] Gao W, Zhao Z, Yu G, Zhou Z, Zhou Y, Hu T, Jiang R, Zhang J. VEGI attenuates the inflammatory injury and disruption of blood-brain barrier partly by suppressing the TLR4/NF-kappaB signaling pathway in experimental traumatic brain injury. Brain Res 2015; 1622: 230-239.

[8] Jayakumar AR, Tong XY, Ruiz-Cordero R, Bregy A, Bethea JR, Bramlett HM, Norenberg MD. Ac-

tivation of NF-kappaB mediates astrocyte swelling and brain edema in traumatic brain injury. J Neurotrauma 2014; 31: 1249-1257.
[9] Liu HD, Li W, Chen ZR, Hu YC, Zhang DD, Shen W, Zhou ML, Zhu L, Hang CH. Expression of the NLRP3 inflammasome in cerebral cortex after traumatic brain injury in a rat model. Neurochem Res 2013; 38: 2072-2083.
[10] McKee CA, Lukens JR. Emerging roles for the immune system in traumatic brain injury. Front Immunol 2016; 7: 556.
[11] Mortezaee K, Khanlarkhani N, Beyer C, Zendedel A. Inflammasome: its role in traumatic brain and spinal cord injury. J Cell Physiol 2018; 233: 5160-5169.
[12] Sung PH, Lee FY, Lin LC, Chen KH, Lin HS, Shao PL, Li YC, Chen YL, Lin KC, Yuen CM, Chang HW, Lee MS, Yip HK. Melatonin attenuated brain death tissue extract-induced cardiac damage by suppressing DAMP signaling. Oncotarget 2018; 9: 3531-3548.
[13] Bao L, Meng Q, Li Y, Deng S, Yu Z, Liu Z, Zhang L, Fan H. C-Kit positive cardiac stem cells and bone marrow-derived mesenchymal stem cells synergistically enhance angiogenesis and improve cardiac function after myocardial infarction in a paracrine manner. J Card Fail 2017; 23: 403-415.
[14] Chang CL, Leu S, Sung HC, Zhen YY, Cho CL, Chen A, Tsai TH, Chung SY, Chai HT, Sun CK, Yen CH, Yip HK. Impact of apoptotic adipose-derived mesenchymal stem cells on attenuating organ damage and reducing mortality in rat sepsis syndrome induced by cecal puncture and ligation. J Transl Med 2012; 10: 244.
[15] Chang CL, Sung PH, Chen KH, Shao PL, Yang CC, Cheng BC, Lin KC, Chen CH, Chai HT, Chang HW, Yip HK, Chen HH. Adipose-derived mesenchymal stem cell-derived exosomes alleviate overwhelming systemic inflammatory reaction and organ damage and improve outcome in rat sepsis syndrome. Am J Transl Res 2018; 10: 1053-1070.
[16] Lee FY, Chen KH, Wallace CG, Sung PH, Sheu JJ, Chung SY, Chen YL, Lu HI, Ko SF, Sun CK, Chiang HJ, Chang HW, Lee MS, Yip HK. Xenogeneic human umbilical cord-derived mesenchymal stem cells reduce mortality in rats with acute respiratory distress syndrome complicated by sepsis. Oncotarget 2017; 8: 45626-45642.
[17] Lin KC, Yip HK, Shao PL, Wu SC, Chen KH, Chen YT, Yang CC, Sun CK, Kao GS, Chen SY, Chai HT, Chang CL, Chen CH, Lee MS. Combination of adipose-derived mesenchymal stem cells (ADMSC) and ADMSC-derived exosomes for protecting kidney from acute ischemia-reperfusion injury. Int J Cardiol 2016; 216: 173-185.
[18] Kim JM, Lee ST, Chu K, Jung KH, Song EC, Kim SJ, Sinn DI, Kim JH, Park DK, Kang KM, Hyung Hong N, Park HK, Won CH, Kim KH, Kim M, Kun Lee S, Roh JK. Systemic transplantation of human adipose stem cells attenuated cerebral inflammation and degeneration in a hemorrhagic stroke model. Brain Res 2007; 1183: 43-50.
[19] Lee ST, Chu K, Jung KH, Kim SJ, Kim DH, Kang KM, Hong NH, Kim JH, Ban JJ, Park HK, Kim SU, Park CG, Lee SK, Kim M, Roh JK. Anti-inflammatory mechanism of intravascular neural stem cell transplantation in haemorrhagic stroke. Brain 2008; 131: 616-629.
[20] Ma X, Qin J, Song B, Shi C, Zhang R, Liu X, Ji Y, Ji W, Gong G, Xu Y. Stem cell-based therapies for intracerebral hemorrhage in animal model: a meta-analysis. Neurol Sci 2015; 36: 1311-1317.
[21] Wang C, Fei Y, Xu C, Zhao Y, Pan Y. Bone marrow mesenchymal stem cells ameliorate neurological deficits and blood-brain barrier dysfunction after intracerebral hemorrhage in spontaneously hypertensive rats. Int J Clin Exp Pathol 2015; 8: 4715-4724.
[22] Hu GW, Li Q, Niu X, Hu B, Liu J, Zhou SM, Guo SC, Lang HL, Zhang CQ, Wang Y, Deng ZF. Exosomes secreted by human-induced pluripotent stem cell-derived mesenchymal stem cells attenuate limb ischemia by promoting angiogenesis in mice. Stem Cell Res Ther 2015; 6: 10.
[23] Soontararak S, Chow L, Johnson V, Coy J, Wheat W, Regan D, Dow S. Mesenchymal stem cells (MSC) derived from induced pluripotent stem cells (iPSC) equivalent to adipose-derived MSC in promoting intestinal healing and microbiome normalization in mouse inflammatory bowel disease model. Stem Cells Transl Med 2018; 7: 456-467.
[24] Roux C, Saviane G, Pini J, Belaid N, Dhib G, Voha C, Ibanez L, Boutin A, Mazure NM, Wakkach A, Blin-Wakkach C, Rouleau M. Immunosuppressive mesenchymal stromal cells derived from human-induced pluripotent stem cells induce human regulatory T cells in vitro and in vivo. Front Immunol 2017; 8: 1991.
[25] Shafa M, Ionescu LI, Vadivel A, Collins JJP, Xu L, Zhong S, Kang M, de Caen G, Daneshmand M, Shi J, Fu KZ, Qi A, Wang Y, Ellis J, Stanford WL, Thebaud B. Human induced pluripotent stem cell-derived lung progenitor and alveolar epithelial cells attenuate hyperoxia-induced lung injury. Cytotherapy 2018; 20: 108-125.
[26] Wu HJ, Yiu WH, Wong DWL, Li RX, Chan LYY, Leung JCK, Zhang Y, Lian Q, Lai KN, Tse HF, Tang SCW. Human induced pluripotent stem cell-derived mesenchymal stem cells prevent adriamycin nephropathy in mice. Oncotarget 2017; 8: 103640-103656.

[27] Ko SF, Chen YT, Wallace CG, Chen KH, Sung PH, Cheng BC, Huang TH, Chen YL, Li YC, Chang HW, Lee MS, Yang CC, Yip HK. Inducible pluripotent stem cell-derived mesenchymal stem cell therapy effectively protected kidney from acute ischemia-reperfusion injury. Oncotarget 2017; 8: 103640-103656.

[28] Qin J, Gong G, Sun S, Qi J, Zhang H, Wang Y, Wang N, Wang QM, Ji Y, Gao Y, Shi C, Yang B, Zhang Y, Song B, Xu Y. Functional recovery after transplantation of induced pluripotent stem cells in a rat hemorrhagic stroke model. Neurosci Lett 2013; 554: 70-75.

[29] Qin J, Ma X, Qi H, Song B, Wang Y, Wen X, Wang QM, Sun S, Li Y, Zhang R, Liu X, Hou H, Gong G, Xu Y. Transplantation of induced pluripotent stem cells alleviates cerebral inflammation and neural damage in hemorrhagic stroke. PLoS One 2015; 10: e0129881.

[30] Moshayedi P, Carmichael ST. Hyaluronan, neural stem cells and tissue reconstruction after acute ischemic stroke. Biomatter 2013; 3.

[31] Moshayedi P, Nih LR, Llorente IL, Berg AR, Cinkornpumin J, Lowry WE, Segura T, Carmichael ST. Systematic optimization of an engineered hydrogel allows for selective control of human neural stem cell survival and differentiation after transplantation in the stroke brain. Biomaterials 2016; 105: 145-155.

[32] Nih LR, Moshayedi P, Llorente IL, Berg AR, Cinkornpumin J, Lowry WE, Segura T, Carmichael ST. Engineered HA hydrogel for stem cell transplantation in the brain: biocompatibility data using a design of experiment approach. Data Brief 2017; 10: 202-209.

[33] Feeney DM, Boyeson MG, Linn RT, Murray HM, Dail WG. Responses to cortical injury: I. Methodology and local effects of contusions in the rat. Brain Res 1981; 211: 67-77.

[34] Flierl MA, Stahel PF, Beauchamp KM, Morgan SJ, Smith WR, Shohami E. Mouse closed head injury model induced by a weight-drop device. Nat Protoc 2009; 4: 1328-1337.

[35] Xu J, Wang H, Ding K, Lu X, Li T, Wang J, Wang C, Wang J. Inhibition of cathepsin S produces neuroprotective effects after traumatic brain injury in mice. Mediators Inflamm 2013; 2013: 187873.

[36] Chang MW, Young MS, Lin MT. An inclined plane system with microcontroller to determine limb motor function of laboratory animals. J Neurosci Methods 2008; 168: 186-194.

[37] Chen YL, Tsai TH, Wallace CG, Chen YL, Huang TH, Sung PH, Yuen CM, Sun CK, Lin KC, Chai HT, Sheu JJ, Lee FY, Yip HK. Intra-carotid arterial administration of autologous peripheral blood-derived endothelial progenitor cells improves acute ischemic stroke neurological outcomes in rats. Int J Cardiol 2015; 201: 668-683.

[38] Yen CH, Tsai TH, Leu S, Chen YL, Chang LT, Chai HT, Chung SY, Chua S, Tsai CY, Chang HW, Ko SF, Sun CK, Yip HK. Sildenafil improves long-term effect of endothelial progenitor cell-based treatment for monocrotaline-induced rat pulmonary arterial hypertension. Cytotherapy 2013; 15: 209-223.

[39] Chang CL, Sung PH, Sun CK, Chen CH, Chiang HJ, Huang TH, Chen YL, Zhen YY, Chai HT, Chung SY, Tong MS, Chang HW, Chen HH, Yip HK. Protective effect of melatonin-supported adipose-derived mesenchymal stem cells against small bowel ischemia-reperfusion injury in rat. J Pineal Res 2015; 59: 206-220.

[40] Chen HH, Lin KC, Wallace CG, Chen YT, Yang CC, Leu S, Chen YC, Sun CK, Tsai TH, Chen YL, Chung SY, Chang CL, Yip HK. Additional benefit of combined therapy with melatonin and apoptotic adipose-derived mesenchymal stem cell against sepsis-induced kidney injury. J Pineal Res 2014; 57: 16-32.

[41] Banjara M, Ghosh C. Sterile neuroinflammation and strategies for therapeutic intervention. Int J Inflam 2017; 2017: 8385961.

[42] Mann DL, Topkara VK, Evans S, Barger PM. Innate immunity in the adult mammalian heart: for whom the cell tolls. Trans Am Clin Climatol Assoc 2010; 121: 34-50; discussion 50-31.

[43] Rubartelli A, Lotze MT. Inside, outside, upside down: damage-associated molecular-pattern molecules (DAMPs) and redox. Trends Immunol 2007; 28: 429-436.

[44] Seong SY, Matzinger P. Hydrophobicity: an ancient damage-associated molecular pattern that initiates innate immune responses. Nat Rev Immunol 2004; 4: 469-478.

[45] Farkas AM, Kilgore TM, Lotze MT. Detecting DNA: getting and begetting cancer. Curr Opin Investig Drugs 2007; 8: 981-986.

[46] Janeway C. Immunogenicity signals 1,2,3 ... and 0. Immunol Today 1989; 10: 283-286.